Analysis of Parametric Oscillatory Instability in Power Recycled LIGO Interferometer

V. B. Braginsky, S. E. Strigin and S. P. Vyatchanin
Faculty of Physics , Moscow State University, Moscow 119992, Russia
e-mail: vyat@hbar.phys.msu.su
(February 7, 2008)

We present the analysis of a nonlinear effect of parametric oscillatory instability in power recycled LIGO interferometer with the Fabry-Perot (FP) cavities in the arms. The basis for this effect is the excitation of the additional (Stokes) optical mode with frequency ω_1 and the mirror elastic mode with frequency ω_m, when the optical energy stored in the main FP cavity mode with frequency ω_0 exceeds the certain threshold and the frequencies are related as $\omega_0 \simeq \omega_1 + \omega_m$. The presence of anti-Stokes modes (with frequency $\omega_{1a} \simeq \omega_0 + \omega_m$) can depress parametric instability. However, it is very likely that the anti-Stokes modes will not compensate the parametric instability completely.

I. INTRODUCTION

The full scale terrestrial interferometric gravitational wave antennae are in process of assembling and tuning at present. One of these antennae (LIGO-I project) sensitivity expressed in terms of the metric perturbation amplitude is projected to achieve the level of $h \simeq 1 \times 10^{-21}$ [1,2]. After the improvement of the isolation from noises in test masses (the mirrors of the 4 km long optical FP cavities) and after increasing the optical power circulating in the resonator up to $W \simeq 830$ kW the sensitivity is expected to reach the value of $h \simeq 1 \times 10^{-22}$ [3]. This value of W corresponds to the energy $\mathcal{E}_0 \simeq 22$ J stored in the FP resonator.

In previous paper [4] we have described the possibly existing effect of pure nonlinear dynamical origin which may cause substantial decrease of the antennae sensitivity or even the antenna disfunction. The essence of this effect is classical parametric oscillatory instability in the FP cavity which modes are coupled with mechanical degree of freedom of the mirror. This effect appears above the certain threshold of the optical energy $\mathcal{E}_0$ when the difference $\omega_0 - \omega_1$ between the frequency ω_0 of the main optical mode (which stores $\mathcal{E}_0$) and the frequency ω_1 of the idle (Stokes) mode is close to the frequency ω_m of the mirror mechanical degree of freedom. The coupling between these three modes appears due to the ponderomotive pressure of the light photons in main and Stokes modes and due to the parametric action of mechanical oscillation on the optical modes. Above the critical value of energy $\mathcal{E}_0$ (dimensionless parameter $\mathcal{R}_0 > 1$, see below) the amplitude of mechanical oscillation will rise exponentially as well as the optical power in the idle (Stokes) optical mode.

In the article [4] we have used a simplified model of this effect in which lumped model of mechanical oscillator had been used and optical modes with gaussian distribution over the cross section had been taken into account. Under these assumptions the parametric oscillatory instability will appear if

$$\frac{\mathcal{R}_0}{\left(1 + \frac{\Delta\omega_1^2}{\delta_1^2}\right)} > 1, \tag{1}$$

$$\mathcal{R}_0 = \frac{\mathcal{E}_0}{2mL^2\omega_m^2}\,\frac{\omega_1\omega_m}{\delta_1\delta_m} = \frac{2\mathcal{E}_0 Q_1 Q_m}{mL^2\omega_m^2}\,. \tag{2}$$

Here m is the value of the order of mirror mass, L is the distance between the FP cavity mirrors, $\Delta\omega_1 = \omega_0 - \omega_1 - \omega_m$, δ_1 and $Q_1 = \omega_1/2\delta_1$ are the relaxation rate and quality factor of the Stokes mode correspondingly, δ_m and $Q_m = \omega_m/2\delta_m$ are relaxation rate and quality factor of the mechanical oscillator.

Recently E. D'Ambrosio and W. Kells [5] have reported that if in the same one dimensional model the anti-Stokes mode (with frequency $\omega_{1\,a} = \omega_0 + \omega_m$) is taken into account then the effect of parametric instability will be substantially dumped or even excluded. In this article we present the analysis based on the model which takes into account several important details of the antenna. This analysis shows that parametric oscillatory instability still may exist.

In section II we present the analysis of one dimensional optical model of antenna in which the so called power recycled mirror is taken into account. In section III important key elements of 3-dimensional approach are used to prove that it is very likely that the anti-Stokes modes will not compensate the oscillatory instability.

II. THE ROLE OF POWER RECYCLING MIRROR IN THE ANTENNA

The design of laser interferometer gravitational wave antenna apart from the two main optical FP cavities also includes the so called power recycling mirror (PRM) which allows to increase the value of $\mathcal{E}_0$ using the same laser input power (see fig. 1).

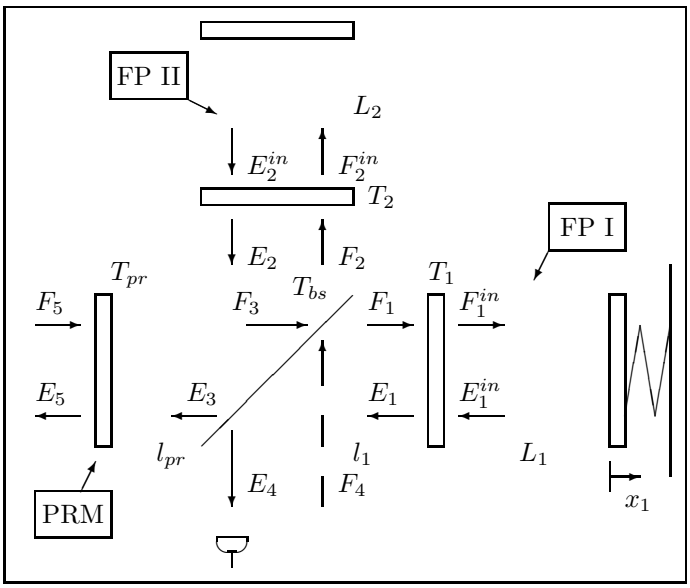

FIG. 1. The scheme of power recycled LIGO interferometer with the Fabry-Perot (FP) cavities in the arms. The end mirror of the FP I cavity is a part of mechanical oscillator. T_{bs} and T_{pr} are transmittances of the beam splitter and power recycling mirror correspondingly, l_1 is the distance between the input mirror of the FP I cavity and the beam splitter, l_{pr} is the distance between the power recycling mirror and the beam splitter, F_i and E_i are the complex amplitudes of travelling optical waves in different parts of interferometer.

The results of calculations presented below are based on the following simplifying assumptions:

- Only one mirror (in the FP I cavity in fig. 1) is movable, it is a part of mechanical oscillator that is considered as lumped one with single mechanical degree of freedom (eigenfrequency ω_m, quality factor $Q_m = \omega_m/2\delta_m$ and mass m which is of the order of the total mirror mass). All other mirrors are assumed to be fixed.

- All mirrors have no optical losses. Both end mirrors of FP cavities have the ideal reflectivity. The input mirrors of the FP cavities are identical and have the finite transmittances $T_1 = T_2 = T = 2\pi L/(\lambda_0 Q_{opt})$ (λ_0 is the optical wavelength, Q_{opt} is the quality factor, L is the distance between the mirrors). The distances $L_1 = L_2 = L$ are equal.

- Only the main (pumped) mode with frequency ω_0 and relaxation rate $\delta_0 = \omega_0/2Q_0$, and Stokes mode with ω_1 and $\delta_1 = \omega_1/2Q_1$ correspondingly are taken into account (Q_0 and Q_1 are the quality factors). It is assumed that $\omega_0 - \omega_1 \simeq \omega_m$.

- Only the main mode is pumped by laser and the value of stored energy $\mathcal{E}_0$ is constant (approximation of constant field).

- In this particular model we do not take into account the possible influence of the anti-Stokes mode.

It is possible to calculate at what level of energy $\mathcal{E}_0$ the Stokes mode and mechanical oscillator become unstable. The origin of this instability can be described qualitatively in the following way: small mechanical oscillations with resonance frequency ω_m modulate the distance L that causes the excitation of optical fields with frequencies $\omega_0 \pm \omega_m$. Therefore, the Stokes mode amplitude will rise linearly in time if time interval is shorter than relaxation time. The presence of two optical fields with frequencies ω_0 and ω_1 will produce the component of ponderomotive force (which is proportional to the square of fields sum) at difference frequency $\omega_0 - \omega_1$. Thus this force will increase the initially small amplitude of mechanical oscillations.

For analysis of parametric instability we have to use two equations for the Stokes mode and mechanical oscillator, and find the conditions when this "feedback" prevails the damping which exists due to the finite values of relaxation in mechanical resonator and in the FP cavity. Note that in resonance $\omega_0 \simeq \omega_1 + \omega_m$ the effect of parametric instability for power recycled LIGO interferometer is larger than for the separate FP cavity because the Stokes wave (at frequency ω_1) emitted from the FP cavity throughout its input mirror is not lost irreversible but returns back due to power recycling mirror, therefore, its interaction is prolonged.

We can write down the field components E_0^{in}, E_1^{in} of the main and Stokes modes inside the FP I cavity correspondingly and the displacement x of mechanical oscillator in rotating wave approximation as:

$$\begin{aligned} E_0^{in} &= A_0[D_0 e^{-i\omega_0 t} + D_0^* e^{i\omega_0 t}], \\ E_1^{in} &= A_1[D_1 e^{-i\omega_1 t} + D_1^* e^{i\omega_1 t}], \\ x &= X e^{-i\omega_m t} + X^* e^{i\omega_m t}, \end{aligned} \tag{3}$$

where D_0 and D_1 are the slowly changing complex amplitudes of the main and Stokes modes correspondingly, and X is the slowly changing complex amplitude of mechanical displacement. Normalizing constants A_0, A_1 are chosen so that energies $\mathcal{E}_{0,1}$ stored in each mode (of the FP I cavity) are equal to $\mathcal{E}_{0,1} = \omega_{0,1}^2 |D_{0,1}|^2/2$. Then one can obtain the equations for slowly changing amplitudes (see details in Appendix A):

$$\begin{aligned} (\partial_t + \delta_1)(\partial_t + \delta_{pr}) D_1^* &= \frac{-iD_0^*\omega_0}{L} \times \\ &\times \left[\partial_t + \delta_{pr} + \frac{\delta_1}{2}\right] \cdot X e^{i\Delta\omega_1 t}, \\ \Delta\omega_1 &= \omega_0 - \omega_1 - \omega_m, \\ \delta_1 = \frac{cT}{4L}, \quad \delta_{pr} &= \frac{T_{pr}\delta_1}{4} \ll \delta_1, \end{aligned} \tag{4}$$

$$(\partial_t + \delta_m)\, X = \frac{iD_0 D_1^* \omega_0 \omega_1}{m\omega_m L} e^{-i\Delta\omega_1 t}. \tag{5}$$

Remind that we assume D_0 to be constant. The additional relaxation rate δ_{pr} describes the relaxation of oscillations in the FP cavity with power recycling mirror.

One can find the solutions of (4, 5) in the following form

$$D_1^*(t) = D_1^* e^{\lambda_1 t}, \quad \lambda_1 = \lambda + i\Delta\omega_1$$
$$X(t) = X\, e^{\lambda t},$$

and write down the characteristic equation:

$$(\lambda + \delta_m) = \frac{\mathcal{R}_0 \delta_1 \delta_m}{\lambda_1 + \delta_1} \left[1 + \frac{\delta_1}{2(\lambda_1 + \delta_{pr})}\right]. \tag{6}$$

(7)

The parametric oscillatory instability will appear if one of the characteristic equation roots real part is positive. Analysis of this equation with assumption

$$\delta_m \ll \delta_{pr} \ll \delta_1,$$

gives the condition of parametric instability (see details in Appendix B):

$$\frac{\mathcal{R}_0}{\left(1 + \frac{\Delta\omega_1^2}{\delta_1^2}\right)} \times \frac{2 + \frac{\delta_1}{\delta_{pr}} + \frac{\Delta\omega_1^2}{\delta_{pr}^2}}{2\left(1 + \frac{\Delta\omega_1^2}{\delta_{pr}^2}\right)} > 1\,. \tag{8}$$

In ultimate resonance case when $\Delta\omega_1 \ll \delta_{pr}$ we obtain the condition of resonance parametric instability:

$$\mathcal{R}_0 \times \left(1 + \frac{\delta_1}{2\delta_{pr}}\right) > 1. \tag{9}$$

It means that the parametric instability takes place at energy $\mathcal{E}_0$ which is smaller than one for the separate FP cavity by the factor of $\sim \frac{\delta_1}{2\delta_{pr}}$.

It is important that factors $\mathcal{R}_0$ and $\frac{\delta_1}{2\delta_{pr}}$ have large numerical values, using the parameters for probe mass fabricated from high quality [8] fused silica that are planned to use in LIGO-II we obtain (see [6] and Appendix D):

$$\mathcal{R}_0 \simeq 6100, \quad \frac{\delta_1}{2\delta_{pr}} \simeq 31\,. \tag{10}$$

It means that if $\Delta\omega_1 \ll \delta_{pr}$ the maximal energy stored in the FP cavity can not exceed the value of about $6100 \times 31 \sim 1.9 \times 10^5$ times *smaller* than one planned for LIGO-II (!).

Note that the estimate of $\mathcal{R}_0$ differs from the estimate presented in [4] because here we use parameters more close to ones planned for LIGO-II. In particular: *(a)* mass is four times greater than in [4]; *(b)* mechanical frequency is assumed to be two times smaller; *(c)* loss angle (and mechanical relaxation rate) is ~ 4 times smaller in accordance with results of Ageev and Penn [8]; *(d)* relaxation rate δ_1 is ~ 6 times smaller.

The probability of the ultimate resonance ($\Delta\omega_1 \ll \delta_{pr}$) is extremely low because the value of $\delta_{pr} \simeq 1.5\ \mathrm{s}^{-1}$ is rather small. In more realistic case when $\Delta\omega_1^2 \gg \delta_1\delta_{pr}$ we obtain the "partial resonance" condition of parametric instability from (8):

$$\frac{\mathcal{R}_0}{2\left(1 + \frac{\Delta\omega_1^2}{\delta_1^2}\right)} > 1\,. \tag{11}$$

It means that in the case when $\delta_1 \gg \Delta\omega_1 \gg \sqrt{\delta_1\delta_{pr}}$ the maximal energy stored in the FP cavity can not exceed the value of about 3050 times *smaller* than one planned for LIGO-II (!). Note that condition (11) differs from the parametric instability condition in the separate FP cavity [4] by the factor of 2 in denominator.

The considered model is the simplest one and more detailed 3-dimensional model of interferometer has to be analyzed. In particular, there are reasons to hope that the danger of parametric instability may be smaller in real interferometer:

- Even in resonance the Stokes and elastic modes may not spatially suit to each other (small overlapping factor).
- The possible presence of the anti-Stokes mode may partially or completely depress the parametric instability.

In the next section we consider both these factors.

III. CONSIDERATION ON THREE-DIMENSIONAL ANALYSIS

It is possible to generalize the above simplified model for the arbitrary elastic mode in the mirror. It has been shown [4] that in this case the constant $\mathcal{R}_0$ in condition (8) should be multiplied by the overlapping factor Λ_1.

In general case when both Stokes and anti-Stokes modes have to be taken into account the characteristic equation may be presented in the following form:

$$\begin{aligned}(\lambda + \delta_m) = {} & \mathcal{R}_0 \delta_1 \delta_m \times \frac{\Lambda_1}{\lambda_1 + \delta_1}\left[1 + \frac{\delta_1}{2(\lambda_1 + \delta_{pr})}\right] - \\ & - \mathcal{R}_0 \delta_1 \delta_m \times \frac{\omega_{1a}}{\omega_1} \times \frac{\Lambda_{1a}}{\lambda_{1a} + \delta_{1a}} \times \\ & \times \left[1 + \frac{\delta_{1a}}{2(\lambda_{1a} + \delta_{pr\,a})}\right], \end{aligned} \tag{12}$$

$$\Lambda_1 = \frac{V\left(\int f_0(\vec{r}_\perp) f_1(\vec{r}_\perp) u_z d\vec{r}_\perp\right)^2}{\int |f_0|^2 d\vec{r}_\perp \int |f_1|^2 d\vec{r}_\perp \int |\vec{u}|^2 dV},$$

$$\Lambda_{1a} = \frac{V\left(\int f_0(\vec{r}_\perp) f_{1a}(\vec{r}_\perp) u_z d\vec{r}_\perp\right)^2}{\int |f_0|^2 d\vec{r}_\perp \int |f_{1a}|^2 d\vec{r}_\perp \int |\vec{u}|^2 dV},$$

$$\lambda_1 = \lambda + i\Delta\omega_1, \quad \Delta\omega_1 = \omega_0 - \omega_1 - \omega_m\,,$$

$$\lambda_{1a} = \lambda + i\Delta\omega_{1a}, \quad \Delta\omega_{1a} = \omega_{1a} - \omega_0 - \omega_m\,.$$

The equation (12) is the generalization of (6). Hereinafter subscript $_1$ corresponds to the Stokes mode and subscript $_{1a}$ to the anti-Stokes mode. Λ_1, Λ_{1a} are the overlapping factors for the Stokes and anti-Stokes modes correspondingly. f_0, f_1 and f_{1a} are the functions of the optical fields distribution in the main, Stokes and anti-Stokes optical modes correspondingly over the mirror surface. Vector $\vec{u}$ is the spatial vector of displacements in the elastic mode, u_z is the component of $\vec{u}$ normal to the mirror surface, $\int d\vec{r}_\perp$ corresponds to the integration over the mirror surface, and $\int dV$ over the mirror volume V.

Analyzing this characteristic equation one can see that the presence of the anti-Stokes mode can considerably depress or even exclude parametric instability. For example, let the main, Stokes and anti-Stokes modes be equidistant and belong to the main frequency sequence $\omega_1 = \pi(K-1)c/L,\ \omega_0 = \pi Kc/L,\ \omega_{1a} = \pi(K+1)c/L$ (K is an integer). In this case $\Delta\omega_1 = \Delta\omega_{1a}$, the main, Stokes and anti-Stokes modes have the same gaussian distribution over the cross section and hence the same overlapping factors: $\Lambda_1 = \Lambda_{1a}$. It means that the second term in the right part of (12) is larger than first term, the *positive* damping introduced into elastic mode by the anti-Stokes mode is greater than *negative* damping due to the Stokes mode, hence the parametric instability is impossible. This case has been analyzed in details in [5].

However, it is worth noting that this situation is possible only for the small part of the total number of optical modes (see fig. 2). Indeed, resonance conditions $\omega_0 \simeq \omega_1 + \omega_m$ can be fulfilled with a relatively high probability for many of the optical Stokes and mirror elastic modes combinations. If we assume the main optical mode to be gaussian with the waist radius of the caustic w_0 (the optical field amplitude distribution in the middle between the mirrors is $\sim e^{-r^2/w_0^2}$)), then the Stokes and anti-Stokes modes are described by generalized Laguerre functions (Gauss-Laguerre beams) and the set of frequency distances between the main and Stokes (anti-Stokes) modes is determined by three integer numbers:

$$\omega_0 - \omega_1 = \frac{\pi c}{L}\left(K - \frac{2(2N+M)}{\pi}\arctan\frac{L\lambda_0}{2\pi w_0^2}\right) \simeq$$
$$\simeq (2.4\,K - 0.66\,N - 0.33\,M)\times 10^5\,\mathrm{s}^{-1}, \quad (13)$$
$$\omega_{1a} - \omega_0 \simeq (2.4\,K_a + 0.66\,N_a + 0.33\,M_a)\times 10^5\,\mathrm{s}^{-1}.$$

where λ_0 is the wavelength, $K = 0 \pm 1, \pm 2\ldots$ is the longitudinal index, $N = 0,\ 1,\ 2\ldots$, and $M = 0,\ 1,\ 2\ldots$ are the radial and angular indices, other numerical parameters are given in Appendix D. We see that full depression of parametric instability takes place only if the Stokes and anti-Stokes modes belong to the main sequence i.e. $M = N = 0$, when $\Delta\omega_1 = \Delta\omega_{1a}$ and the Stokes and anti-Stokes modes have equal spatial gaussian distribution. Such modes obviously present the small part of the total optical modes number. Indeed for $K = 1,\ N = M = 0$ we have from (13) $\omega_0 - \omega_1 \simeq 2.4\times 10^5$ sec^{-1}. However, our numerical calculations show (see below) that the lowest elastic mode has the frequency of about nine times smaller: $\omega_{m\,\mathrm{lowest}} \simeq 0.28\times 10^5$ sec^{-1} and *only* within the range between 0.28×10^5 sec^{-1} and 1.6×10^5 sec^{-1} there are more than 50 (!) elastic modes and each of them has to be carefully considered as possible candidate for parametric instability.

For the case when the Stokes and anti-Stokes modes do not belong to the main sequence (non zero numbers N and M) the frequencies of the suitable Stokes and anti-Stokes modes are not equidistant from the main mode (i.e. $\Delta\omega_1 \neq \Delta\omega_{1a}$) and have different spatial distributions (i.e. $\Lambda_1 \neq \Lambda_{1a}$). Illustration of this is given in fig. 2. For the shown Stokes mode (left to the main mode) there is no suitable anti-Stokes mode (it should be located right to the main one). In this case one can use the approximate condition for the parametric instability (see details of approximations in Appendix C):

$$\frac{\mathcal{R}_0\Lambda_1}{\left(1+\frac{\Delta\omega_1^2}{\delta_1^2}\right)}\times\frac{2+\frac{\delta_1}{\delta_{pr}}+\frac{\Delta\omega_1^2}{\delta_{pr}^2}}{2\left(1+\frac{\Delta\omega_1^2}{\delta_{pr}^2}\right)} - \quad (14)$$
$$-\frac{\mathcal{R}_0\Lambda_{1a}}{\left(1+\frac{\Delta\omega_{1a}^2}{\delta_{1a}^2}\right)}\,\frac{\omega_{1a}}{\omega_1}\times\frac{2+\frac{\delta_{1a}}{\delta_{pr\,a}}+\frac{\Delta\omega_{1a}^2}{\delta_{pr\,a}^2}}{2\left(1+\frac{\Delta\omega_{1a}^2}{\delta_{pr\,a}^2}\right)} > 1\,.$$

Here the second term in the right part describes the influence of the anti-Stokes mode.

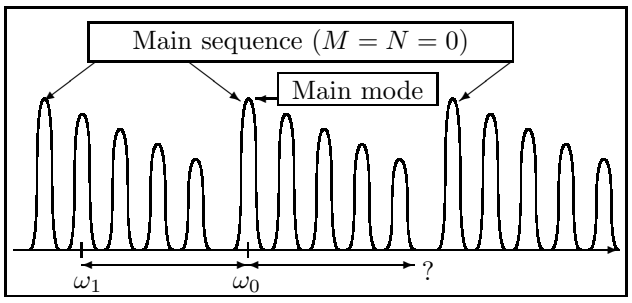

FIG. 2. Schematic structure of optical (Laguer-Gauss) modes in the FP cavity. The modes of the main frequencies sequence are shown by higher peaks. It is shown that Stokes mode with frequiency ω_1 may not have suitable anti-Stokes mode (it is denoted by question-mark).

The above consideration for lossless mirrors can be generalized for mirrors with losses. Analyzing the more important case when only the FP cavity mirrors have losses with loss coefficient $R \ll T$ for each of them we can easily show all previous formulas to be valid taking the following substitutions into account:

$$\delta_1 \Rightarrow \delta_{1R} = \delta_1(1+\eta), \quad \eta = \frac{2R}{T} \ll 1, \quad (15)$$

$$\delta_{pr} \Rightarrow \delta_{pr\,R} = \left(\frac{T_{pr}}{4} + \eta\right)\delta_1\,. \quad (16)$$

We see that in the case $\eta \ll T_{pr}/4$ all formulas does not change, in the case of $1 \gg \eta \gg T_{pr}/4$ the condition of the ultimate resonance changes but the condition of partial resonance remains unchanged. For LIGO-II the losses are negligible (it is planned that $R \simeq 5$ ppm, $\eta \simeq 2\times 10^{-3} \ll T_{pr}/4$).

The account of losses is important when we consider optical modes with high indices $M,\ N$ because their diffractional losses increases for higher indices $M,\ N$. We have numerically calculated the equivalent loss coefficient $R_{M,\,N}$ describing the diffractional losses on each mirror and have found that

$$\eta_{\mathrm{dif}} = \frac{2R_{M,\,N}}{T} < \frac{T_{pr}}{4} \simeq 0.015, \quad \text{if } \ 2N + M \leq 6,$$
$$\eta_{\mathrm{dif}} < 1, \quad \text{if } \ 2N + M \leq 9,$$

We see that there is a wide range of indices M, N which must be taken into account when analyzing parametric instability. Note that even for the case $\eta_{\rm dif} > 1$ the parametric instability may also be possible due to the large numeric value of factor $\mathcal{R}_0$.

Using the Femlab program package we have numerically calculated the first 50 elastic modes frequencies and spatial distributions in the cylindric mirror fabricated from fused silica (parameters are listed in Appendix D). These frequencies lied within the range between 28000 $\sec^{-1}$ and 164000 $\sec^{-1}$. We have estimated the errors $\Delta\omega_m$ of these frequencies comparing the data obtained with different total number of nodes ($N_n \simeq 1135$ and $N_n \simeq 3777$): $\Delta\omega_m \simeq 500 \cdots 4000$ $\sec^{-1}$ (the error increases for elastic modes at higher frequencies). Such error is unacceptably large because in order to determine the ultimate resonance in power recycled interferometer the error have to be $\Delta\omega_m \ll \delta_{pr} \simeq 1.5$ $\sec^{-1}$ or in the case of "partial resonance" $\Delta\omega_m \ll \delta_1 \simeq 94$ $\sec^{-1}$.

It is worth noting that the frequency density of elastic modes rapidly increases at higher frequencies. In particular, the mean distance $\Delta\omega_{md}$ between the elastic modes frequencies can be estimated as follows:

$$\Delta\omega_{md} \simeq \frac{2\omega^3_{m\,\rm lowest}}{\pi\omega^2_m}\,,$$

and it is equal to $\Delta\omega_{md} \simeq 100$ $\sec^{-1} \simeq \delta_1$ even at $\omega_m = 3.8\times10^5$ $\sec^{-1}$. It means that practically for each elastic mode with frequency higher than 3.8×10^5 $\sec^{-1}$ there exists the Stokes mode with small detuning: $\Delta\omega_1 < \delta_1$ ("partial resonance"). However, the same speculations can also be referred to the anti-Stokes modes and hence the accurate calculation of overlapping factors $\Lambda_1,\ \Lambda_{1\,a}$ is required for each of the elastic modes.

Even in the case of parametric resonance the overlapping factor Λ_1 may be zero (for example, elastic mode and the Stokes mode can have different dependence on azimuth angle). However, it is important to take into account that only the elastic mode attached to the mirror axis in contrast to the optical mode which can be shifted from the mirror axis due to non-perfect optical alignment. Hence, the overlapping factor must depend on distance Z between the center of mirror and the center of the main optical mode distribution over the mirror surface. It means that Λ_1 may be zero for $Z = 0$ but nonzero for $Z \neq 0$. Therefore, the numerical analysis of the mode structure should evidently include the case when $Z \neq 0$. Note that there is a proposal to use special shift Z of the laser beam of about several centimeters from the mirror axis in order to decrease thermal suspension noise [9].

Due to the necessity to decrease the level of thermoelastic and thermorefractive noises [10,12,11,7] the size of the light spot on the mirror surface is likely to be substantially larger and the light density distribution in the spot is not likely to be gaussian (the "mexican hat" modes [7]) to evade substantial diffractional losses. The optical modes which are complementary to such a "mexican hat" main mode have the frequencies more close to the main mode than given by equation (13), and the probability to be entrapped into the parametric instability is higher. Thus the estimates presented above for gaussian optical modes may be regarded only as the first approximation in which the use of analytical calculations is still possible.

IV. CONCLUSION

Summing up the above calculations and considerations we have to conclude that the effect of parametric oscillatory instability is a potential danger for the gravitational wave antennae with powerful laser pumping. From our point of view, to estimate correctly this danger it is necessary to implement the following subprograms of researches:

1. To calculate numerically the values of eigenfrequencies ω_m for lower elastic modes with relative errors of at least $10^{-4}\cdots10^{-3}$. It is not an easy task because the error in standard schemes of finite elements calculations rises as square of ω_m. It is necessary to keep in mind that these calculations will play a role of introductory ones because it is likely that in LIGO-II non-gaussian mode distribution of light will be used (so called "mexican hat" mode) and, correspondingly, it will be necessary to calculate numerically all spectrum of "mexican hat" modes.

2. At the same time the numerical analysis can not solve the problem completely because the fused silica pins and suspension fibers will be attached to the mirror. This attachment will change the elastic modes frequency values (and may be also the quality factor and distribution). For example, assuming the pin mass of about $\Delta m \simeq 80$ g one can estimate that frequency shift may be about

$$\Delta\omega_{m\,pin} \leq \pm\frac{\omega_m}{1\times10^5\ \sec^{-1}} \times \frac{\Delta m}{2m} \simeq \pm100\ \sec^{-1},$$

   i.e. about the value of δ_1 (!). In addition, the unknown Young modulus and fused silica density inhomogeneity (we estimate it may be of about $10^{-3}\cdots10^{-2}$) will additionally limit the numerical analysis accuracy. Thus we have to conclude that *the direct measurements* of eigenfrequency values, distribution and quality factors for several hundreds of elastic modes for each mirror of FP cavity are *inevitably* necessary.

3. When more "dangerous" candidates of elastic and Stokes modes will be known their undesirable influence can be possibly decreased. Perhaps, it can be done by *accurate* small change of mirror shape or by introducing low noise damping [13].

4. The last stage of this program should be presented by the *direct tests* of the optical field behavior with smooth increase of the input optical power: it will

be possible to register the appearance of the photons at the Stokes modes and the rise of the Q_m in the corresponding elastic mode while the power W in the main optical mode is below the critical value.

We think that the parametric oscillatory instability effect can be overcome in the laser gravitational antennae after these detailed investigations.

ACKNOWLEDGEMENTS

This work was supported in part by NSF and Caltech grant PHY0098715, by Russian Ministry of Industry and Science and by Russian Foundation of Basic Researches.

APPENDIX A: POWER RECYCLED INTERFEROMETER

In this Appendix we deduce the equations (4, 5).

1. Internal FP Cavities

For the fourier components of complex slowly changing amplitudes in general case we have obvious expressions (see notations in fig. 1):

$$F_1^{in}(\Omega) = \frac{2i\delta_1\, F_1(\Omega)}{\sqrt{T_1}\,(\delta_1 - i\Delta\omega - i\Omega)}, \quad \delta_{1,2} = \frac{cT_{1,2}}{4L_{1,2}}, \tag{A1}$$

$$E_1(\Omega) = -F_1(\Omega)\,\frac{\delta_1 + i\Delta\omega + i\Omega}{\delta_1 - i\Delta\omega - i\Omega}\,. \tag{A2}$$

One can obtain the similar formulas for the second FP cavity:

$$F_2^{in}(\Omega) = \frac{2i\delta_2\, F_2(\Omega)}{\sqrt{T_2}\,(\delta_2 - i\Omega)}, \tag{A3}$$

$$E_2(\Omega) = -F_2(\Omega)\,\frac{\delta_2 + i\Omega}{\delta_2 - i\Omega}\,. \tag{A4}$$

2. The Mean and Small Amplitudes

Let us introduce the mean amplitude and small amplitude (denoted by small letters). For example, for amplitude in the FP I cavity it means: $F_1^{in} = \mathcal{F}_1^{in} + f_1^{in}$.

Let us also assume that $\delta_2 = \delta_1$, and now we keep in mind that

$$\Delta\omega = \frac{\omega_1 x}{L_1}\,. \tag{A5}$$

Then the mean amplitudes are written as follows:

$$\mathcal{F}_1^{in} = \frac{2i}{\sqrt{T_1}}\,\mathcal{F}_1, \quad \mathcal{E}_1 = -\mathcal{F}_1, \tag{A6}$$

$$\mathcal{F}_2^{in} = \frac{2i}{\sqrt{T_1}}\,\mathcal{F}_2, \quad \mathcal{E}_2 = -\mathcal{F}_2\,. \tag{A7}$$

Rewriting the equations (A2 and A4) we find the small amplitudes:

$$(\mathcal{E}_1 + e_1) \times \big(\delta_1 - i\Delta\omega - i\Omega\big) = -\big(\mathcal{F}_1 + f_1\big)\,\big(\delta + i\Delta\omega + i\Omega\big), \tag{A8}$$

$$e_1 = -f_1\,\Gamma_0 - \mathcal{F}_1\,\Gamma_1, \quad e_2 = -f_2\Gamma_0\,, \tag{A9}$$

$$\Gamma_0 = \frac{\delta_1 + i\Omega}{\delta_1 - i\Omega}, \quad \Gamma_1 = \frac{2i\Delta\omega}{\delta_1 - i\Omega}\,. \tag{A10}$$

3. Beam Splitter

Assuming that $T_{bs} = 1/2$ one can write the following:

$$F_1 e^{-i\phi_1} = \frac{1}{\sqrt{2}}\big(iF_3 + F_4\big), \quad F_2 = \frac{1}{\sqrt{2}}\big(F_3 + iF_4\big),$$
$$E_4 = \frac{1}{\sqrt{2}}\big(iE_2 + E_1 e^{i\phi_1}\big), \quad E_3 = \frac{1}{\sqrt{2}}\big(E_2 + iE_1 e^{i\phi_1}\big)\,.$$

Here $\phi_1 = kl_1$ is the wave E_1 phase shift due to length path l_1 between the FP cavity and the beam splitter. We assume that $\phi_1 = \pi/2$ and analogous phase shift ϕ_2 (for the wave E_2) is equal to zero. Then one can obtain for the mean amplitudes the following:

$$\mathcal{F}_1 = \frac{-\mathcal{F}_3}{\sqrt{2}}, \quad \mathcal{E}_1 = \frac{\mathcal{F}_3}{\sqrt{2}}, \tag{A11}$$

$$\mathcal{F}_2 = \frac{\mathcal{F}_3}{\sqrt{2}}, \quad \mathcal{E}_2 = \frac{-\mathcal{F}_3}{\sqrt{2}} \tag{A12}$$

$$\mathcal{E}_4 = 0, \quad \mathcal{E}_3 = -\mathcal{F}_3, \tag{A13}$$

Small amplitudes are equal to:

$$f_1 = \frac{-f_3 + if_4}{\sqrt{2}}, \quad f_2 = \frac{f_3 + if_4}{\sqrt{2}}, \tag{A14}$$
$$e_4 = f_4\,\Gamma_0 + \frac{i\mathcal{F}_3\Gamma_1}{2}, \quad e_3 = -f_3\Gamma_0 - \frac{\mathcal{F}_3\Gamma_1}{2}.$$

4. Power Recycling Mirror

We have the following expressions:

$$F_3 e^{-i\phi_{pr}} = i\sqrt{T_{pr}}F_5 + \sqrt{1 - T_{pr}}E_3 e^{i\phi_{pr}}, \tag{A15}$$

$$E_5 = i\sqrt{T_{pr}}E_3 e^{i\phi_{pr}} + \sqrt{1 - T_{pr}}F_5, \tag{A16}$$

$$\phi_{pr} = \frac{\big(\omega_0 + \Delta\omega_{pr} + \Omega\big)l_{pr}}{c}. \tag{A17}$$

Using (A13) and assuming that the PR cavity is in resonance: $\exp(i\omega_0 l_{pr}/c) = i$ (i.e. $\omega_0 l_{pr}/c = \pi/2 + 2\pi n$, n is an integer) one can obtain:

$$\mathcal{F}_3 \simeq \frac{-2\mathcal{F}_5}{\sqrt{T_{pr}}}, \quad \mathcal{E}_3 \simeq \frac{2\mathcal{F}_5}{\sqrt{T_{pr}}}\,, \tag{A18}$$

$$f_3 A_3 \simeq -f_5\sqrt{T_{pr}} + \frac{\mathcal{F}_3\Gamma_1}{2}, \tag{A19}$$

$$A_3 \simeq 1-\Gamma_0+\Gamma_0\frac{T_{pr}}{2}\left(1-\frac{i\big(\Delta\omega_{pr}+\Omega\big)}{\tilde{\delta}_{pr}}\right), \quad \text{(A20)}$$

$$\tilde{\delta}_{pr}=\frac{cT_{pr}}{4L_{pr}}.$$

The value of $\tilde{\delta}_{pr} \gg |\Delta\omega_{pr}+\Omega|$ and hence one can rewrite (A20) as follows:

$$A_3 \simeq 1-\Gamma_0+\Gamma_0\frac{T_{pr}}{2}=2\,\frac{\delta_{pr}-i\Omega}{\delta_1-i\Omega}, \quad \text{(A21)}$$

$$\delta_{pr}=\frac{T_{pr}\delta_1}{4}. \quad \text{(A22)}$$

And finally, for f_3 one can obtain the following:

$$f_3 \simeq \frac{\delta_1-i\Omega}{2(\delta_{pr}-i\Omega)}\left(-f_5\sqrt{T_{pr}}+\frac{\mathcal{F}_3\Gamma_1}{2}\right). \quad \text{(A23)}$$

Using (A16)we will have:

$$\mathcal{E}_5=-\mathcal{F}_5, \quad \text{(A24)}$$

$$e_5=\sqrt{T_{pr}}\left(f_3\Gamma_0+\frac{\mathcal{F}_3\,\Gamma_1}{2}\right)+f_5. \quad \text{(A25)}$$

5. The Small Variational Amplitude in the FP I Cavity

In order to calculate the small amplitude f_1 one can rewrite equation (A1) using (A14) and (A19) assuming that small amplitudes f_4 and f_5 describing vacuum fluctuations of the input waves are zero:

$$\left(\mathcal{F}_1^{in}+f_1^{in}\right)\times(\delta_1-i\Delta\omega-i\Omega)= \quad \text{(A26)}$$

$$=\frac{i\sqrt{2}\delta_1\,(-\mathcal{F}_3-f_3+if_4)}{\sqrt{T_1}},$$

$$\mathcal{F}_1^{in}=\frac{2i\mathcal{F}_1}{\sqrt{T_1}}=-\frac{i\sqrt{2}\,\mathcal{F}_3}{\sqrt{T_1}}=\frac{2i\sqrt{2}\,\mathcal{F}_5}{\sqrt{T_1T_{pr}}}, \quad \text{(A27)}$$

$$f_1^{in}\,(\delta_1-i\Omega)\;=i\Delta\omega\,\mathcal{F}_1^{in}- \quad \text{(A28)}$$

$$-\frac{i\sqrt{2}\,\delta_1}{\sqrt{T_1}}\left(\frac{\delta_1-i\Omega}{2(\delta_{pr}-i\Omega)}\right)\mathcal{F}_3\,\frac{\Gamma_1}{2}. \quad \text{(A29)}$$

It can be rewritten using (A27) as:

$$f_1^{in}\,(\delta_1-i\Omega)\,(\delta_{pr}-i\Omega)=i\mathcal{F}_1^{in}\Delta\omega\left[\delta_{pr}-i\Omega+\frac{\delta_1}{2}\right]. \quad \text{(A30)}$$

6. Time Domain

Now it seems that one can make in (A30) the following substitution:

$$\mathcal{F}_1^{in}\to D_0e^{-i(\omega_0-\omega_1)t}, \quad \Delta\omega\to\frac{\omega_1}{L_1}\,X^*e^{i\omega_m t}.$$

However, such substitution will be incorrect, because the equation for the fourier transform of complex amplitude has not contain time-dependent terms. The correct form of this equation is the following:

$$f_1^{in}(\Omega)\,(\delta_1-i\Omega)\,(\delta_{pr}-i\Omega)= \quad \text{(A31)}$$

$$=iD_0^{in}\,X^*(\Omega-\Delta\omega_1)\frac{\omega_1}{L_1}\left[\delta_{pr}-i\Omega+\frac{\delta_1}{2}\right].$$

Now one can obtain time domain equivalent of (A31) applying inverse fourier transform:

$$(\partial_t+\delta_1)\,(\partial_t+\delta_{pr})\,f_1^{in}(t)= \quad \text{(A32)}$$

$$=iD_0^{in}\,e^{-i\Delta\omega_1 t}\,\frac{\omega_1}{L_1}\times\left[\partial_t+\delta_{pr}-i\Delta\omega_1+\frac{\delta_1}{2}\right]X^*(t)=$$

$$=iD_0^{in}\,\frac{\omega_1}{L_1}\times\left[\partial_t+\delta_{pr}+\frac{\delta_1}{2}\right]X^*(t)\,e^{-i\Delta\omega_1 t}.$$

The last equation is the complex conjugate to (4) where:

$$f_1^{in}\to D_1.$$

7. Equation for Elastic Oscillations

For elastic displacement we have the following equation:

$$\partial_t^2x+2\delta_m\partial_tx+\omega_m^2x=\frac{F_{pm}}{m}, \quad \text{(A33)}$$

$$F_{pm}=\frac{2S}{c}\,\frac{(E_0+E_1)^2}{4\pi}\simeq$$

$$\simeq\frac{S}{\pi c}\Big(\mathcal{F}_0^{in}(f_1^{in})^*e^{-i(\omega_0-\omega_1)t}+ \quad \text{(A34)}$$

$$+(\mathcal{F}_0^{in})^*f_1^{in}e^{i(\omega_0-\omega_1)t}\Big),$$

where S is the cross section of light beam, c is the light speed. Introducing the slow amplitudes for displacement x:

$$x(t)=X(t)\,e^{-i\omega_m t}+X^*(t)\,e^{i\omega_m t},$$

one can obtain the following:

$$\partial_tX+\delta_mX=\frac{iS}{2\pi cm\omega_m}\mathcal{F}_0^{in}(f_1^{in})^*e^{-i\Delta\omega_1 t}, \quad \text{(A35)}$$

$$\Delta\omega_1=\omega_0-\omega_1-\omega_m. \quad \text{(A36)}$$

This equation coincides with (5) after the substitutions, listed below:

$$f_1^{in}\to D_1, \quad \mathcal{F}_0\to D_0.$$

APPENDIX B: SOLUTION OF THE CHARACTERISTIC EQUATION (8)

In this Appendix we obtain the instability condition (8) from the characteristic equation (6).

Let us write down the the solution of equation (6) as sum of real and imaginary part:

$$\lambda = a + ib\,.$$

The condition of instability is $a > 0$. Thus substituting $\lambda = ib$ into (6) one can find two equations (introducing notations A and B):

$$\delta_m = \underbrace{\mathcal{R}_0\delta_1\delta_m \times \frac{\delta_1}{(b+\Delta\omega_1)^2+\delta_1^2}}_{A} \times \underbrace{\left[1 + \frac{\delta_1\delta_{pr} - (b+\Delta\omega_1)^2}{2[(b+\Delta\omega_1)^2+\delta_{pr}^2]}\right]}_{B}, \tag{B1}$$

$$b = -\mathcal{R}_0\delta_1\delta_m \times \frac{(b+\Delta\omega_1)}{(b+\Delta\omega_1)^2+\delta_1^2} \times \underbrace{\left[1 + \frac{\delta_1(\delta_1+\delta_{pr})}{2[(b+\Delta\omega_1)^2+\delta_{pr}^2]}\right]}_{C} = \tag{B2}$$

$$= -\frac{\delta_m(b+\Delta\omega_1)C}{\delta_1 B}\,. \tag{B3}$$

Using the last equation one can formally express b as:

$$b = -\Delta\omega_1\ \frac{\delta_m C}{\delta_1 B}\Big/\left(1+\frac{\delta_m C}{\delta_1 B}\right),$$

$$\frac{C}{B} = \frac{2\delta_{pr}^2 + \delta_1(\delta_1+\delta_{pr}) + 2(b+\Delta\omega_1)^2}{2\delta_{pr}^2 + \delta_1\delta_{pr} + (b+\Delta\omega_1)^2}\,. \tag{B4}$$

It is obvious from the last expression that

$$2 < \frac{C}{B} < \frac{\delta_1}{\delta_{pr}}$$

for *any* value of $(b+\Delta\omega_1)$. Hence one can conclude from (B4) that $|b| \ll \Delta\omega_1$ (remind that $\delta_m \ll \delta_1$) and equation (B1) can be simplified as follows:

$$\delta_m = \mathcal{R}_0\delta_1\delta_m \times \frac{\delta_1}{(\Delta\omega_1^2+\delta_1^2)} \times \times \frac{\delta_{pr}(\delta_1+2\delta_{pr}) + \Delta\omega_1^2}{2[\Delta\omega_1^2+\delta_{pr}^2]}\,. \tag{B5}$$

Now rewriting this equation one can easily obtain the condition of parametric instability (8).

APPENDIX C: SOLUTION OF THE CHARACTERISTIC EQUATION (14)

In this Appendix using some approximation we deduce the instability condition (14) from the characteristic equation (12).

We write down the the solution of this equation as a sum of real and imaginary parts anew:

$$\lambda = a + ib$$

and assume $a = 0$. So substituting $\lambda = ib$ into (12) and extracting real and image parts we can write two equations:

$$\delta_m = \underbrace{\mathcal{R}_0\delta_1\delta_m \times \frac{\delta_1\Lambda_1}{(b+\Delta\omega_1)^2+\delta_1^2}}_{A_1} \times \underbrace{\left[1 + \frac{\delta_1\delta_{pr} - (b+\Delta\omega_1)^2}{2[(b+\Delta\omega_1)^2+\delta_{pr}^2]}\right]}_{B_1} - \underbrace{\mathcal{R}_0\delta_1\delta_m\,\frac{\omega_{1a}}{\omega_1} \times \frac{\delta_{1a}\Lambda_{1a}}{(b+\Delta\omega_{1a})^2+\delta_{1a}^2}}_{A_{1a}} \times \underbrace{\left[1 + \frac{\delta_{1a}\delta_{pr\,a} - (b+\Delta\omega_{1a})^2}{2[(b+\Delta\omega_{1a})^2+\delta_{pr\,a}^2]}\right]}_{B_{1a}} = \tag{C1}$$

$$= \underbrace{A_1B_1}_{\delta_{m\,1}} - \underbrace{A_{1a}B_{1a}}_{\delta_{m\,1a}}, \tag{C2}$$

$$b = -\mathcal{R}_0\delta_1\delta_m \times \frac{\Lambda_1(b+\Delta\omega_1)}{(b+\Delta\omega_1)^2+\delta_1^2} \times \underbrace{\left[1 + \frac{\delta_1(\delta_1+\delta_{pr})}{2[(b+\Delta\omega_1)^2+\delta_{pr}^2]}\right]}_{C_1} + \mathcal{R}_0\delta_1\delta_m\,\frac{\omega_{1a}}{\omega_1} \times \frac{\Lambda_{1a}(b+\Delta\omega_{1a})}{(b+\Delta\omega_{1a})^2+\delta_{1a}^2} \times \underbrace{\left[1 + \frac{\delta_{1a}(\delta_{1a}+\delta_{pr\,a})}{2[(b+\Delta\omega_{1a})^2+\delta_{pr\,a}^2]}\right]}_{C_{1a}} = \tag{C3}$$

$$= -A_1C_1\,\frac{b+\Delta\omega_1}{\delta_1} + A_{1a}C_{1a}\,\frac{b+\Delta\omega_{1a}}{\delta_{1a}}\,. \tag{C4}$$

Using notations (C2) this equation can be rewritten as:

$$b = -\frac{\delta_{m\,1}C_1}{\delta_1 B_1} \times (b+\Delta\omega_1) + \frac{\delta_{m\,1a}C_{1a}}{\delta_{1a}B_{1a}} \times (b+\Delta\omega_{1a})\,,$$

and one can formally express b as:

$$b = \frac{\left(-\Delta\omega_1\,\frac{\delta_{m1}C_1}{\delta_1 B_1} + \Delta\omega_{1\,a}\,\frac{\delta_{m1\,a}C_{1\,a}}{\delta_{1\,a}B_{1\,a}}\right)}{\left(1+\frac{\delta_{m1}C_1}{\delta_1 B_1} - \frac{\delta_{m1\,a}C_{1\,a}}{\delta_{1\,1}B_{1\,a}}\right)}. \tag{C5}$$

Using definitions (C1, C3) it is easy to prove that

$$2 < \frac{C_1}{B_1} < \frac{\delta_1}{\delta_{pr}} \quad \text{or} \quad \frac{2\delta_{m1}}{\delta_1} < \frac{\delta_{m1}C_1}{\delta_1 B_1} < \frac{\delta_{m1}}{\delta_{pr}}\,,$$

$$2 < \frac{C_{1a}}{B_{1a}} < \frac{\delta_{1a}}{\delta_{pr\,a}} \quad \text{or} \quad \frac{2\delta_{m1\,a}}{\delta_a 1} < \frac{\delta_{m1\,a}C_{1\,a}}{\delta_{1\,a}B_{1\,a}} < \frac{\delta_{m1\,a}}{\delta_{pr\,a}}.$$

Now assuming that

$$\frac{\delta_{m\,1}}{\delta_{pr}} \ll 1, \qquad \frac{\delta_{m\,1a}}{\delta_{pr\,a}} \ll 1\,, \tag{C6}$$

we can conclude that

$$|b| \ll \Delta\omega_1,\ \Delta\omega_{1a}. \tag{C7}$$

Then the parametric instability condition (14) can be easily obtained from (C1).

It is worth noting that inequalities (C6) are the key assumption for deduction of the PI condition (14). These inequalities obviously correspond to the case when values $\delta_{m1} = A_1 B_1$ and $\delta_{m1\,a} = A_{1a} B_{1a}$ are not very close to each other. In order to understand how close they can be let us assume that

$$\delta_{m1\,a} = \delta_{m1}(1-\epsilon), \quad \epsilon \ll 1,$$

and try to estimate theminimal value of ϵ. From (C6) one can obtain $\delta_{m1} \simeq \delta_{m1\,a} \simeq \delta_m/\epsilon$. Hence the inequalities (C6) are equivalent to:

$$\frac{\delta_m}{\epsilon\delta_{pr}} \ll 1\,. \tag{C8}$$

Using parameters of LIGO-II (see Appendix D) we have estimates $\delta_m \simeq 1\times10^{-3}$ sec^{-1}, $\delta_{pr} \simeq 1$ sec^{-1}. Hence one can conclude that for values of $\epsilon \geq 10^{-2}$ the inequalities (C6) fulfill.

APPENDIX D: NUMERICAL PARAMETERS

For interferometer we use parameters planned for LIGO-II. More details see in [6].

$$\begin{array}{llll} \omega_0 &= 2\times10^{15}\ \text{sec}^{-1}, & w_0 &= 5.5\ \text{cm}, \\ T &= 5\times10^{-3}, & L &= 4\times10^5\ \text{cm}, \\ T_{pr} &= 6\times10^{-2}, & l_{pr} &\simeq 10\ \text{m}, \\ \delta_1 &\simeq 94\ \text{sec}^{-1}, & \delta_{pr} &\simeq 1.5\ \text{sec}^{-1}, \\ W &= 830\ \text{kW}, & \mathcal{E}_0 &\simeq 2.2\times10^8\ \text{erg} \end{array} \tag{D1}$$

Here W is the power circulating inside FP cavity ($\mathcal{E}_0 = \frac{2LW}{c}$). We assume that cylindric mirror (with radius R, height H and mass m) is fabricated from fused silica with angle of structural losses $\phi = 1.2\times10^{-8}$ [8]:

$$\begin{array}{llll} R &= 19.4\ \text{cm}, & H &= 15.4\ \text{cm}, \\ m &= 40\ \text{kg}, & \rho &= 2.2\ \text{g/cm}^3, \\ E &= 7.2\times10^{11}\ \frac{\text{erg}}{\text{cm}^3}, & \sigma &= 0.17, \\ \phi &= 1.2\times10^{-8}, & \delta_m &= \omega_m\phi/2. \end{array} \tag{D2}$$

Here E is Young's modulus, σ is Poison ratio. It is useful to calculate factor $\mathcal{R}_0$ for these parameters and elastic mode frequency $\omega_m = 1\times10^5$ sec^{-1}:

$$\mathcal{R}_0 = \frac{\mathcal{E}_0}{2mL^2\omega_m^2}\,\frac{\omega_1\omega_m}{\delta_1\delta_m} = \frac{\mathcal{E}_0\omega_1}{mL^2\omega_m^2\phi\,\delta_1} \simeq 6\,100$$

[1] A. Abramovici *et al.*, *Science* **256**(1992)325.
[2] A. Abramovici *et al.*, *Physics Letters* **A218**, 157 (1996).
[3] Advanced LIGO System Design (LIGO-T010075-00-D), Advanced LIGO System requirements (LIGO-G010242-00), available in http://www.ligo.caltech.edu .
[4] V. B. Braginsky, S. E. Strigin, and S. P. Vyatchanin, *Physics Letters* **A287**, 331 (2001); gr-qc/0107079;
[5] E. D'Ambrosio and W. Kells, to be published in *Physics Letter A*. LIGO-T020008-00-D, available in http://www.ligo.caltech.edu .
[6] http://www.ligo.caltech.edu/∼ligo2/scripts/12refdes.htm
[7] V. B. Braginsky, E. d'Ambrosio, R. O'Shaughnessy, S. E. Strigin, K. Thorne, and S. P. Vyatchanin, reports on LSC Meetings: Baton Rouge, LA, 16 March 2001 and Hanford, WA, 15 August 2001: LIGO documents G010151-00-R and G010333-00-D (http//:www.ligo.caltech.edu/).
[8] A. Yu. Ageev, S. D. Penn, private communications.
[9] V. B. Braginsky, Yu. Levin and S. P. Vyatchanin, *Meas. Sci. Technol* **10** (1999), 598-606.
[10] V. B. Braginsky, M. L. Gorodetsky, and S. P. Vyatchanin, *Physics Letters* **A264**, 1 (1999); cond-mat/9912139;
[11] Yu. T. Liu and K. S. Thorne, submit to *Phys. Rev. D.*
[12] V. B. Braginsky, M. L. Gorodetsky, and S. P. Vyatchanin, *Physics Letters*, **A 271**, 303-307 (2000).
[13] V. B. Braginsky and S. P. Vyatchanin, *Physics Letters A*, **293** (2002) 228-234.